Comparing a MWIR and LWIR polarimetric imager for surface swimmer detection

ARTICLE *in* PROCEEDINGS OF SPIE - THE INTERNATIONAL SOCIETY FOR OPTICAL ENGINEERING · MAY 2008

Impact Factor: 0.2 · DOI: 10.1117/12.785010

4 AUTHORS, INCLUDING:

John Harchanko
Polaris Sensor Technologies
10 PUBLICATIONS **15** CITATIONS

SEE PROFILE

Comparing a MWIR and LWIR polarimetric imager for surface swimmer detection

John S. Harchanko, Larry Pezzaniti, David Chenault, Graham Eades
of Polaris Sensor Technologies, Inc., Huntsville, AL, 35801

ABSTRACT

Previously, we have investigated the use of Long-Wave Infra-Red (LWIR) polarimetric imaging for the detection of surface swimmers in a maritime environment. While better contrast and longer range are expected with Mid-Wave Infra-Red (MWIR) polarimetric imaging, the cost of such a system is higher than a polarimetric imager operating in the LWIR due to the advent of higher-performance micro-bolometer imaging arrays. The actual performance of a MWIR polarimetric imager to detect a person in the water is presented. A comparative analysis of system cost between MWIR and LWIR systems is also discussed.

Keywords: polarimetry, polarimetric imaging, person in water, surface swimmer detection, search and rescue

1. INTRODUCTION

Imaging polarimetry covers a broad class of cameras that utilizes polarizing filters to quantify the orientation of the electro-magnetic field reflected or emitted from a scene and imaged onto a pixilated sensor. The polarization measurement may be done for each pixel or a group of pixels but for this paper corresponds to a single pixel. In its simplest form, imaging polarimetry can be accomplished by taking two recordings with two different orientations of a linear polarizer. The equipment is available to the average amateur photographer. The linear polarizer oriented at some angle, θ, filters the orthogonal state and if n images are collected for some $\Delta\theta$ (such that $\Delta\theta = 2\pi/n$, where n is suitably large enough; e.g. n>6), then a sinusoidal modulation will be evident in those sub-regions of the image that are, to some degree, polarized. The degree of polarization, from 0 to 1, is directly related to the depth of modulation so that completely unpolarized sub-regions undergo no modulation throughout the rotation of the linear polarizer.

To completely characterize the linear polarization state, the polarimetric image is represented by a three element vector, the "partial" Stokes vector, for every pixel. The partial Stokes vector consists of the pixel radiance, the degree of horizontal polarization, and the degree of 45-degree polarization (a "full" Stokes vector requires one more element which is the degree of circular polarization). While a panchromatic camera also measures three quantities for each pixel, red, green, and blue, an imaging polarimeter can substantially improve the target/subject contrast far beyond the standard RGB camera.[1] The Stokes vector, first instroduced by G.G. Stokes in 1852, is useful for describing partially polarized light and is defined as

$$\mathbf{S} = \begin{bmatrix} s_0 \\ s_1 \\ s_2 \\ s_3 \end{bmatrix} = \begin{bmatrix} \left\langle |E_x|^2 + |E_y|^2 \right\rangle \\ \left\langle |E_x|^2 - |E_y|^2 \right\rangle \\ 2\,\mathrm{Re}\left\langle E_x E_y^* \right\rangle \\ -2\,\mathrm{Im}\left\langle E_x E_y^* \right\rangle \end{bmatrix} \propto \begin{bmatrix} I_0 + I_{90} \\ I_0 - I_{90} \\ I_{45} - I_{135} \\ I_L - I_R \end{bmatrix}, \tag{1}$$

where E is the electric field and I is the radiance collected by the camera equipped with a linear polarizer with its orientation given by the subscript in degrees. The I_L and I_R refer to the radiance collected by the camera if it were equipped with a left and right circular polarizer. The first element of the Stokes vector, S_0, is referred to as the radiance image and this is exactly the same image as that produced by a standard panchromatic black and white camera. The remaining Stokes elements are sometimes normalized by the S_0 image so that each element represents a degree of a particular polarization state. In this paper, we utilize both the normalized S_1 and S_2 as well as the radiance S_1 and S_2

Polarization: Measurement, Analysis, and Remote Sensing VIII, edited by David B. Chenault,
Dennis H. Goldstein, Proc. of SPIE Vol. 6972, 697211, (2008) · 0277-786X/08/$18 · doi: 10.1117/12.785010

images (e.g., the un-normalized images as presented in Equation 1) and will differentiate between the two. We will also present the Degree Of Linear Polarization or DOLP, ranging from 0 to 1, which is given by

$$DOLP = \frac{\sqrt{S_1^{\,2} + S_2^{\,2}}}{S_0} \tag{2}$$

We have previously reported[2] on a "first-look" at using a LWIR polarimetric imager to locate a surface swimmer and how the increased signal to background of the resulting polarimetric images can be utilized for object detection and classification. Since that time, Polaris Sensor Technologies, Inc., has completed development of an MWIR polarimetric imager and has collected data from the same location, under similar circumstances, to that of the LWIR polarimetric data. In this paper, we will present the architecture of the two instruments, re-examine the LWIR polarimetric data via quantitative analysis so that a direct comparison with the MWIR instrument can be performed, and, finally, we will present a comparative analysis of cost and performance.

2. LWIR IMAGING POLARIMETER

Figure 1. Long Wave Imaging Polarimeter.

The LWIP is a partial Stokes polarimeter that uses a rapidly rotating half-wave retarder to modulate the polarization signal. The half-waver retarder is an element constructed with enough birefringence to provide half a wave of retardance between two orthogonal states of the electric field; the "fast" and "slow" axes, so named for their respective low and high indices of refraction. The half-wave retarder will rotate the incoming plane of polarization depending upon the angle between the incoming electric field and the retarder's fast axis. For example, if a linear polarization state oriented at 0º, is incident upon a half-wave retarder whose fast axis is oriented at some angle θ, then the linear state will exit the half-wave plate having been rotated by 2θ. A practical problem to incorporating this element in the optical train is that any wedge angle between the front and back surface of the retarder will shift the image by some fraction of a pixel. Some researchers have suggested that anything more than $1/4^{th}$ or even a $1/10^{th}$ of a pixel will seriously affect the accuracy of polarization measurement near object edges. In order to avoid or minimize this shift, the retarder is placed at an intermediate image plane located at or near the front focal plane of a relay lens. A relay lens is then implemented to project this image onto the Focal Plane Array (FPA) of the camera. A static linear polarizer that serves as an analyzer to determine the incoming polarization orientation is located very close to the FPA. A picture of the instrument is shown in Figure 1 and the optical layout is shown in Figure 2.

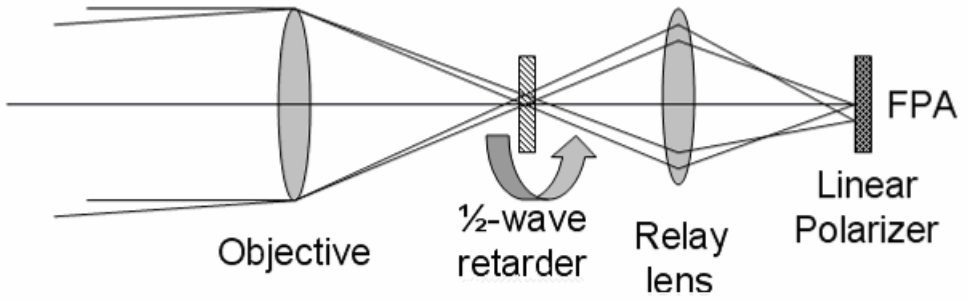

Figure 2. Concept design for the long wave imaging polarimeter.

The sensing plane is of Mercury Cadmium Telluride (HgCdTe) responsive from 8 microns to 11.5 microns; a spectral filter covering the band from 8 microns to 9.5 microns limits the overall wavelength range. The camera was operated at 80 Hz frame rate with a polarimetric frame rate of 5 Hz. The system captures 16 images per revolution of the retarder with the retarder rotating at 5 Hz, thus giving the overall 80 Hz camera frame rate.

Reliable polarimetric data requires both a radiometric and a polarimetric calibration. A non-uniformity correction (NUC) corrects for pixel to pixel responsivity and offsets that are inherent in all FPA's and gives radiometrically correct intensity data. Polarimetric calibration requires the measurement of a minimum of four polarization states and must be sufficient to fully characterize the system response to arbitrary input polarization states. The system response to the calibration states is formulated as a data reduction matrix[3] that provides a computationally efficient approach for producing degree of polarization and Stokes images from the set of raw input images.

On July 24, 2004, the LWIP was transported to Smith Lake, Alabama, to collect data from which we could determine the efficacy of using imaging polarimetry to automatically detect and classify objects on the surface of the water.

3. MWIR DIVISION OF APERTURE IMAGING POLARIMETER

For imaging polarimeters that take multiple images sequentially in time, such as a rotating polarization element system, both the sensor platform and scene must be still while the sequence of images is being captured to within sub-pixel. A simple approach to reduce motion effects is a faster data acquisition system but this necessarily puts an upper limit on integration time of individual frames. In addition, there are practical limits on how fast a polarization optic can be rotated or modulated.

Figure 3. MWIR division of aperture imaging polarimeter

Another solution is to acquire the polarization data simultaneously on a single focal plane array (FPA) or multiple FPAs. Several polarimeter designs have been proposed to measure polarization simultaneously.[4] The division of aperture imaging polarimeter presented here, and shown in Figure 3 has a unique lens design which duplicates a single image formed by a standard objective onto four quadrants of a single FPA..[5] Figure 4 shows an example of 4 images taken from the imaging polarimeter. Each image measures a different linear polarization state at 0, 45, 90, 135 degrees orientation. The images have $1/10^{th}$ pixel registration and are subtracted, (after appropriate calibration multipliers are applied) to observe the linear Stokes polarization content of the image. The resolution of the entire array is 640x512. After data reduction, the resolution of a polarimetric image is approximately 220x220.

Figure 5 shows the concept design for the Division of Aperture Imaging Polarimeter. A standard Camera objective lens is used to form an image of the object onto the field stop. The field-stop and relay optics are contained inside of a vacuum Dewar operating at 77k. The collimation optic forms an image of the Objective lens aperture onto the mini-lens array such that the light incident on the objective lens is evenly divided across the four mini-lens elements. Each mini-lens elements forms an image of the object onto the FPA. A polarizer is placed after each mini-lens to measure a different polarization state across the object. For this polarimeter design a set of four linear polarizers are used at orientations 0, 45, 90 and 135 degrees. Alternatively, other polarization elements can be used to measure circular polarization states as well. For our purposes measuring, linear polarization states is sufficient.

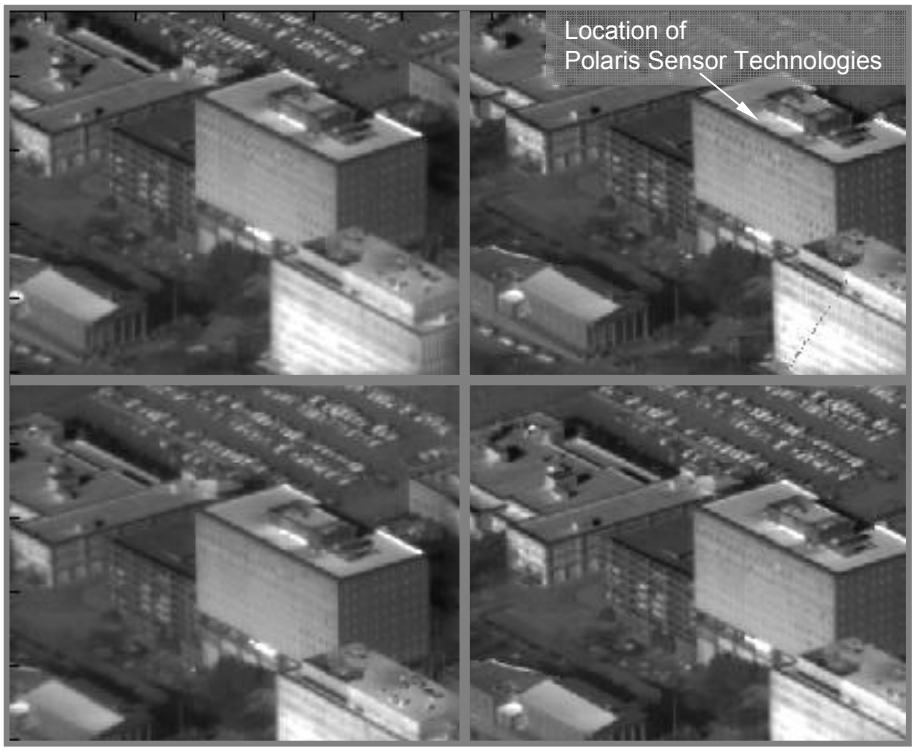

Figure 4. Sample image taken with the division of aperture imaging polarimeter.

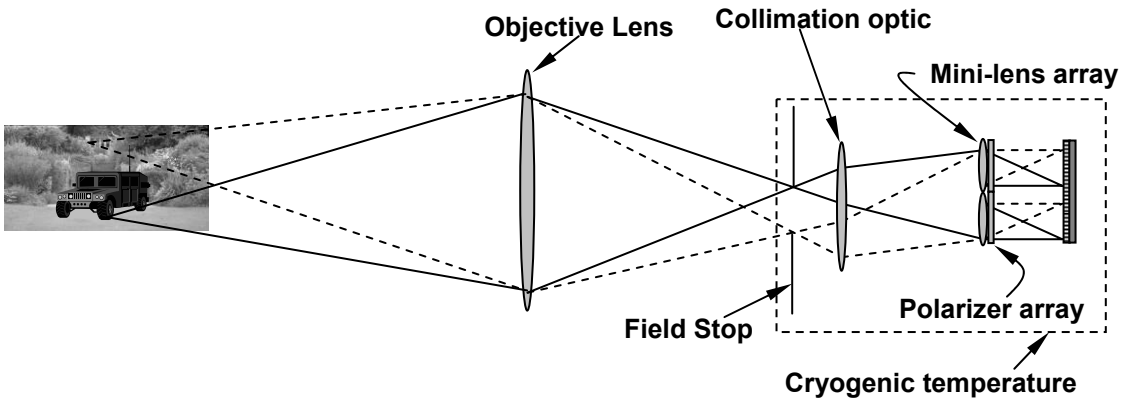

Figure 5. Concept design for Division of Aperture Imaging Polarimeter

4. SAMPLE IMAGE DATA

Some sample data from the LWIR imaging polarimeter is shown in Figure 6. There is a one-to-one correlation between images meaning that any pixel coordinate is mapped exactly to the same pixel coordinate in any of the four images. The scene is of two swimmers whose heads are clearly visible in the radiance S0 image as two bright circles. One of the swimmers is wearing a swim mask. Next to the two swimmers is some flotsam which consists of a crumpled one gallon plastic milk container and a small rectangular Styrofoam cooler. The most intuitive image is the S0 image, although some very interesting information is contained in the totality of the images such that one can determine the wave slope information from this data. The wave slope information is obtained by calculating two angles to describe the surface normal of each wave facet. Each facet corresponds to a single pixel. The first angle of the surface normal for a given pixel is determined by calculating the orientation of the linear state and the second angle of the surface normal is given by the degree of linear polarization[6].

One should begin to suspect this is the case by close examination of the Styrofoam cooler which appears as a dark rectangle on the left hand side of the radiance S0 image. Notice its appearance in the normalized S2 image; the faces on each side of the cooler are visible due to the change in polarization orientation.

In the normalized S1 image, the cooler and the two swimmer's heads have only a very small degree of horizontal polarization while the surrounding water has a negative degree of horizontal polarization. The negative sign simply indicates that the water surface has a strong vertically-polarized component to the reflected and emitted light. Although some materials in this wavelength region (8.5μm-9.0μm) are good emitters (such as the skin, hair, and wetsuit of a swimmer), smooth water can be a strong reflector depending on the viewing angle.

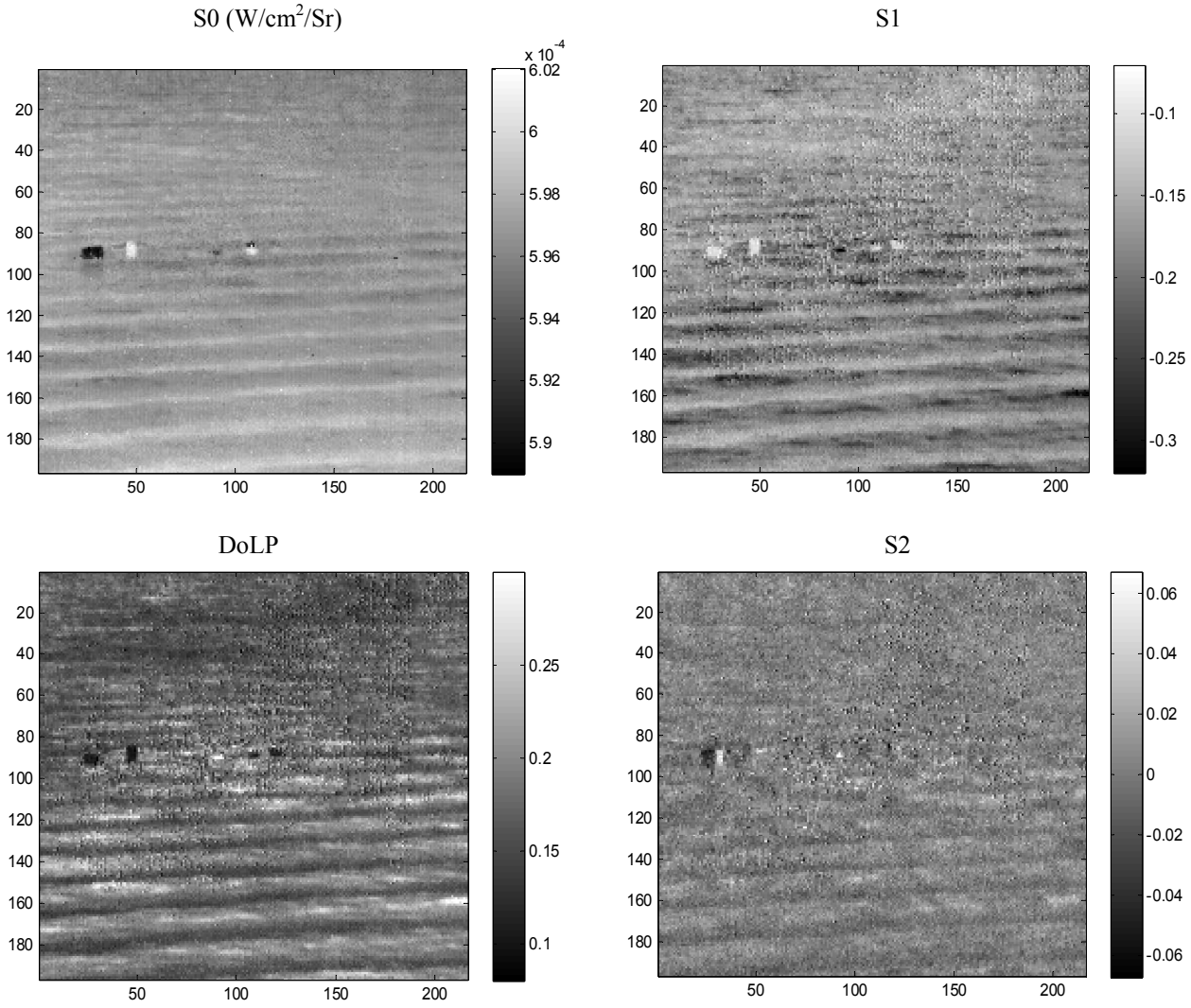

Figure 6. LWIR Imaging Polarimeter. Clockwise from upper left: radiance S0, normalized S1, normalized S2, and DoLP.

Sample data from the MWIR imaging polarimeter is shown in Figure 7. This is the first frame from a series of 1,600 images taken at 88Hz. A swimmer's head is seen slightly up and to the right of center. At the very top of each image, the wake from a boat is seen. The boat was used to generate background waves for the swimmer in order to make the scene more closely resemble an application of this technology to port and harbor security. This data was collected at the same location as the long-wave and the subject is located at nearly the same distance from the camera.

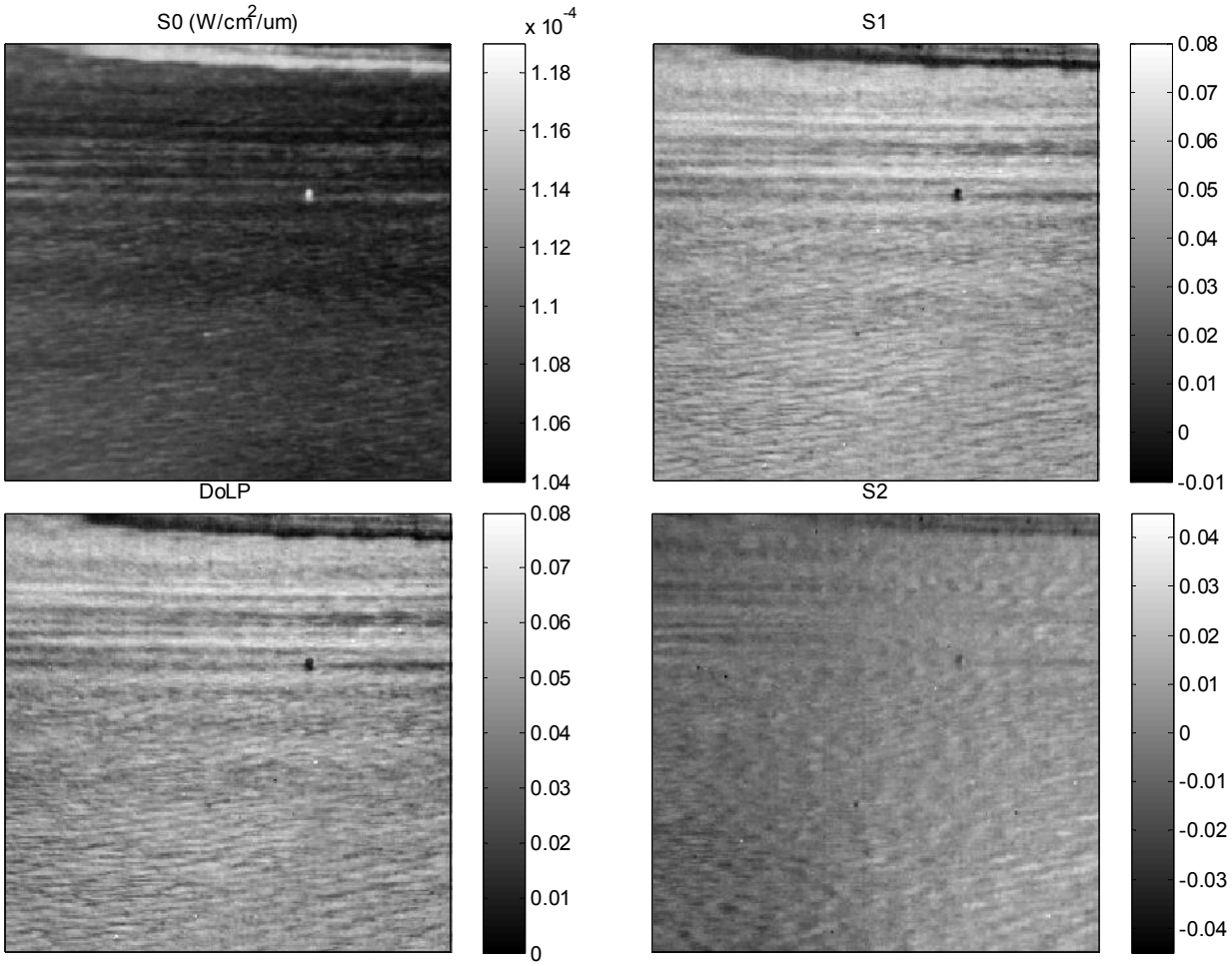

Figure 7. MWIR Imaging Polarimeter. Clockwise from upper left: radiance S0, normalized S1, normalized S2, DoLP.

5. **DATA ANALYSIS**

The data files are stored on the local hard drive of each computer and include the raw data from the camera in addition to the calibration data. This allows for post processing where necessary in order to produce the Stokes vector images, a sample of which has been provided in the prior section. The goal of the data analysis was to determine if it was possible to utilize the Stokes vector images in order to increase the contrast between the swimmer's head and the water and, if so, to what extent. It was also desirable to maximize the visibility of the swimmer's head and to determine if this was a local or global maximum.

When trying to determining the best possible method of data analysis, we must shed the concept of the Stokes vector as being the only method of representing the data; the sample images given in the above section are the default data product given by the polarimeter software. Recall that the Stokes vector components are calculated from I_0, I_{45}, I_{90}, and I_{135} so that the equations may be reversed and given the normalized s_1 and s_2 components,

$$\begin{aligned} I_0 &= \tfrac{1}{2} S_0 (1 + s_1), \\ I_{45} &= \tfrac{1}{2} S_0 (1 + s_2), \\ I_{90} &= \tfrac{1}{2} S_0 (1 - s_1), \\ I_{135} &= \tfrac{1}{2} S_0 (1 - s_2). \end{aligned} \qquad (3), (4), (5), (6)$$

The problem can now be simply reduced to finding the best possible linear combination of these components. To perform this optimization, a composite image is made such that

$$comp\_image = qI_0 + rI_{45} + sI_{90} + tI_{135}, \tag{7}$$

where q, r, s, t are limited to the following values: -1, 0, +1. This produces 81 cases, each of which is scored by a merit function, so that the best values for q, r, s, and t can be found. A simple signal to background ratio for the merit function is insufficient to cover all cases since the radiance (W/cm^2/Sr) of the swimmer's head in the composite image can be near zero. This will produce signal to background ratios approaching 0, even though there is sufficient contrast with the background for an image processing algorithm to easily extract the swimmer from the background. For this reason, we use the visibility formula as a basis for the merit function so that

$$merit = \left| \frac{|I_s| - |I_B|}{|I_s| + |I_B|} \right|, \tag{8}$$

where I_S is the average radiance from the swimmer's head and I_B is the average background radiance. The background radiance is defined as a five-pixel border surrounding the swimmer's head. We use the absolute value because in many of these images, the I_S is close to zero and of the opposite sign from I_B; otherwise, merit functions larger than unity would result which is a nonsensical result.

In each of the images, the general location of the swimmer is known which allows a convolution to using a top-hat kernel to easily find the pixels containing the swimmer's head. This general area is represented as a sub-set of the entire image. An image mean and standard deviation are calculated for the image sub-set. The threshold of the resulting image from the convolution is set to the mean plus four times the standard deviation. This is a fairly typical method for extracting a subject from a background. However, due to the various combinations resulting in *comp_image* (see Equation 7), we must check for the highest convolution result using four similar kernels. The four kernels are a top-hat, an inverse top-hat, a top-hat minus one, and an inverse top-hat plus one. A top-hat kernel is being defined as zero everywhere except for the object shape and size that we are looking for where it is one. In our case, we are looking for a 4x4 pixel area, so our kernel is 5x5 of zeros with the central 4x4 of ones. An inverse top-hat the top-hat just described multiplied by minus one.

Once the subject pixels are known, finding the background pixels and calculating the average radiance of the swimmer's head and immediate background is straightforward. An example of the results using this method is shown in Figure 8 and Figure 9. The signal level is shown as a solid line and the local background level is shown as a dashed line.

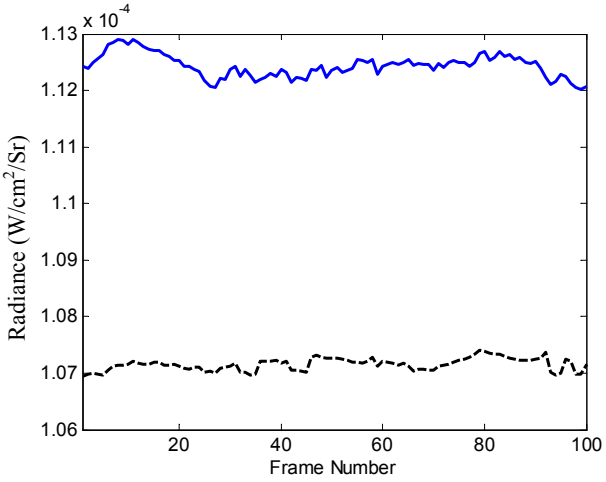

Figure 8. MWIR S0 radiance of "swimmer with waves." Signal mean = 1.137E-4 (solid). Background mean = 1.074E-4 (dashed). Visibility = 2.819E-2.

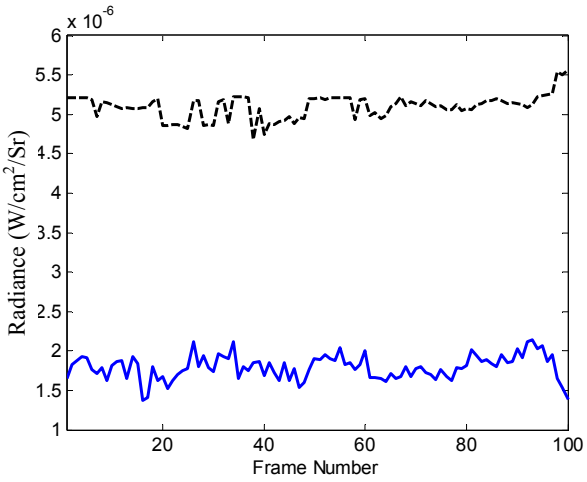

Figure 9. MWIR S1 radiance of "swimmer with waves." Signal mean = 1.793E-6 (solid). Background mean = 5.099E-6 (dashed). Visibility = -4.796E-1.

6. **RESULTS**

In order to ensure that the merit function described in Equation 8 is representative of the whole image sequence, we averaged I_S and I_B over 100 frames taken from the beginning of the sequence using the MWIR polarimetric data.

From the 81 cases produced from our approach to the analysis as described above, there emerged 16 sets of values that scored equally as the highest (the next highest scored more than an order of magnitude lower) according to the visibility merit function of Equation 8. Half of this set consisted of duplicate values in which

$$[q, r, s, t] = -1[q, r, s, t] \tag{9}$$

The top eight unique values for q, r, s, and t for Equation 7 that produce the highest visibility of the swimmer's head compared to the five-pixel border of the local background using Equation 8 are given in Table 1, in row order. Note that the S_1 radiance image is in row 4 but from Equation 9, this scored the same merit function as the (+)S1 radiance image. Similarly, the S_2 radiance image is scored in row 5. To put these merit scores into perspective, the S_0 radiance image (produced by all standard, non-polarimetric cameras) scores a merit of just 2.79×10^{-2}! This would correspond to a vector of [1 0 1 0] using the notation of Equation 10.

Table 1. Top eight unique linear combinations of I_0, I_{45}, I_{90}, and I_{135}.

q_{I_0}	$r_{I_{45}}$	$s_{I_{90}}$	$t_{I_{135}}$	*merit*	*comment*
1	1	−1	−1	0.904	$\approx DoLP$
1	0	0	−1	0.904	$\approx \frac{1}{2} S_1$
0	1	−1	0	0.904	$\approx \frac{1}{2} S_2$
1	0	−1	0	0.792	$\equiv S_1$
0	1	0	−1	0.738	$\equiv S_2$
1	−1	0	0	0.612	$\approx \frac{1}{2} S_1$
1	−1	−1	1	0.612	$= S_1 - S_2$
0	0	1	−1	0.612	$\approx -\frac{1}{2} S_2$

For comparison, the elements by themselves yield the visibility merit scores shown in Table 2. Note that the highest visibility of the swimmer's head is given for a linear polarizer oriented at 90 degrees. This suppresses the horizontal polarization of the water. Comparing the two tables, it is clear that the best visibility is obtained when subtracting the proper images; an order of magnitude increase in the visibility is possible.

Table 2. Merit (visibility) scores for the elements I_0, I_{45}, I_{90}, I_{135}.

q_{I_0}	$r_{I_{45}}$	$s_{I_{90}}$	$t_{I_{135}}$	*merit*
1	0	0	0	$1.606E-2$
0	1	0	0	$2.550E-2$
0	0	1	0	$4.756E-2$
0	0	0	1	$3.216E-2$

To gain a qualitative understanding, it is instructive to examine the S1 and S2 radiance images alongside the S0 radiance image as shown in Figure 10. Note that the merit function for the S2 radiance image will vary as a function of lateral image position due to the coupling of the horizontal component as the plane of incidence shifts from the center of the image.

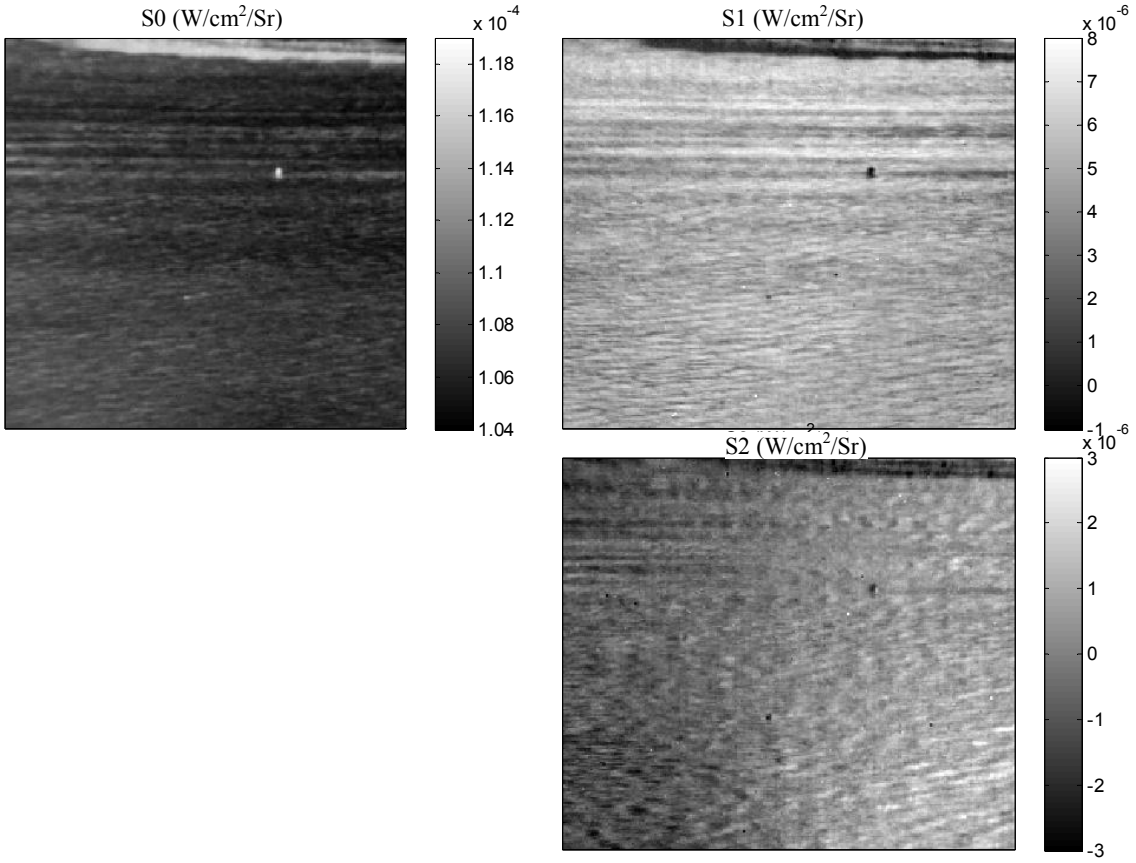

Figure 10. S1 and S2 radiance images shown with the S0 radiance image.

This coupling is simple consequence of 3D geometry; as one moves off-center, the angle of polarization rotates slightly from 0º (the S1 state), even though the camera does not, and couples into the S2 state. This is the reason that the left half of the S2 state is mainly negative while the right half is mainly positive. The effect on the merit function is that at the center of the image, the merit function will trend to zero while at the right edge, it will be a local maximum and at the left edge, it will be a local minimum. (This is the reason why in Table 2, the I_{45} and the I_{135} do not give the same merit function result.) Conversely, the S1 image will yield the same merit function value regardless of the location of the swimmer's head within the image and is therefore a much more robust discriminator. In fact, any linear combination that uses the I_{45} or the I_{135} will not give a target-location independent visibility and thus, to obtain the most robust discriminator, we should rely on only the vertical and horizontal states.

To evaluate the MWIR versus the LWIR polarimetric imager, we have chosen to utilize the radiance S1 image for the reasons discussed above; namely, it produces the highest possible visibility of the swimmer's head and the visibility is expected to be constant regardless of the swimmer's location within the image. The LWIR polarimetric data that was collected in 2004 consists of only 10 polarimetric frames while the MWIR data collected in 2007 consists of 1600 polarimetric frames. A polarimetric frame refers to the S0, S1, and S2 elements of the Stokes vector.

While the location, Smith Lake located in northern Alabama, is the same for both cameras and the swimmer is located at approximately the same distance, the time of year, time of day, atmospheric conditions, etc., are all different. Table 3 summarizes the various test conditions. These conditions will allow the estimation of polarimetric sky conditions to determine the orientation of the reflected component from the water surface. In both instances, the camera was pointed at a bearing of 100 degrees, was 20 feet above the water, and the subject was located approximately 450 feet lateral distance.

Table 3. Summary of various test conditions.

	LWIR Polarimetry	MWIR Polarimetry
Date	24-Jul-04	19-Sep-07
Sky	Hazy	Clear
Air Temp	95º F	75º F
Water Temp	92º F	80º F
Rel Humidity	>80%	60%
Start Time	11:00 AM	1:00 PM
End Time	2:00 PM	3:00 PM
Zenith Start	19.6º	37.3º
Azimuth Start	137.4º	213.0º
Zenith End	31.6º	56.3º
Azimuth End	249.1º	245.5º

Given the differences between not only the cameras and their respective tradeoffs, but also considering the test conditions, it is difficult to make a direct comparison. While the performance of the two cameras is shown within the same table, see Table 4, the intention is to show only the improvement in visibility that is possible with polarimetry. For the LWIR, the improvement is almost two orders of magnitude while the improvement for the MWIR band is nearly a factor of 20. The negative value of the S1 radiance should not be a concern; this simply means that the radiance of the I_{90} image is larger than the radiance of the I_0 image. In a like manner, the negative value of the visibility should not be a concern; this only means that the swimmer's head has more similar radiance between the I_{90} and I_0 images than the background. Therefore, the software to perform automatic image segmentation would be optimized to find portions of the image that are significantly darker than the surrounding area. Due to the increased visibility, this will be a much easier task when using the S1 radiance image.

Table 4. Visibility improvement of S1 radiance over the S0 (standard radiance) images for both the LWIR and MWIR Polarimetric Cameras.

	LWIR Polarimetric Camera		MWIR Polarimetric Camera	
	S0 (Std. Radiance)	**S1 Radiance**	**S0 (Std. Radiance)**	**S1 Radiance**
No. Frames Averaged	10	10	100	100
Background (W/cm^2/Sr)	5.97E-04	-9.84E-05	1.07E-04	4.88E-06
Signal (W/cm^2/Sr)	6.01E-04	-6.02E-05	1.13E-04	5.67E-07
Merit	***2.76E-03***	***2.41E-01***	***2.79E-02***	***7.92E-01***

7. CONCLUSIONS

We have shown that when looking for a particular object within a scene, the proper metric for evaluating the performance of a standard camera to that of a polarimetric camera is to compute the visibility of the object compared to its local background. A standard signal-to-background ratio is insufficient and produces skewed results. Furthermore, to obtain the maximum visibility given the I_0, I_{45}, I_{90}, and I_{135} images, we have also shown that the S1 radiance image gives the highest possible visibility. The polarimetric image gives a much higher visibility than is possible using a standard LWIR or MWIR camera, see Table 4. Improvements in the object's visibility of at least an order of magnitude can conservatively be expected when implementing polarimetric imaging.

The final question is the issue of cost. The MWIR division of aperture polarimetric camera requires a specialized lens design and custom lens components. This expense, added to the cost of a 3-5μm camera from Santa Barbara Focal Plane, brings the total cost to $250k. The LWIR camera used to collect the data in 2004 is no longer considered the best solution for a port and harbor security or search and rescue application. Polaris Sensor Technologies, Inc., has applied recent advancements in micro-bolometer technology to the field of polarimetric imaging and has designed, built, tested, and delivered the division of amplitude LWIR polarimetric camera shown in Figure 11.

Figure 11. Microbolometer-based LWIR Polarimetric Camera

This camera uses two micro-bolometer cameras located behind a polarizing beamsplitter. The beamsplitter orientation is controlled by the knob shown on the right side of the camera. In its state shown, the camera collects the I_0 and I_{90} images necessary for computation of the S1 radiance image. By positioning the knob at the other extreme position, the camera can also collect the I_{45} and the I_{135} images necessary for computation of the S2 radiance image. Unlike the LWIR polarimetric camera utilized in 2004 for this paper, this newer camera collects the I_0 and I_{90} images simultaneously. This is an advantage when the scene is dynamic such as would be encountered for a port and harbor security or search and rescue operation. The cost of this camera is approximately $60k.

REFERENCES

[1] Tyo, J.S., Goldstein, D.H., Chenault, D.B., Shaw, J.A., "Review of passive imaging polarimetry for remote sensing applications," Applied Optics, vol. 45 (issue 22), pp 5453-5469 (2006).

[2] Harchanko, J.S., Chenault, D.B., Farlow, C., Spradley, K., "Detecting a surface swimmer using long wave infared imaging polarimetry (Invited Paper)," Proc. SPIE 5780, Photonics for Port and Harbor Security, pp 138-144 (2005).

[3] Lompado, A., Chenault, D. B., Cabot, E. R., Fetrow, M., "Handheld polarimeter for phenomenology studies," Proc. SPIE 5432, Polarization Analysis and Measurement IV, (2004).

[4] Farlow, C.A., Chenault, D.B., Pezzaniti, J.L., Spradely, K.D., Gulley, M.G., "Imaging polarimeter development and applications," Proc. SPIE 4481, Polarization Analysis and Measurement IV, pp.118-125 (2002).

[5] Pezzaniti, J.L., Chenault, D.B., "A division of aperture MWIR imaging polarimeter," Proc. SPIE 5888, Polarization Science and Remote Sensing II, pp. U1-U12 (2005).

[6] Pezzaniti, J.L., Schultz, H.J., Roche, M.E., Reinhardt, J.E., "Four camera complete Stokes imaging polarimeter," Proc. SPIE 6972, Polarization: Measurement, Analysis, and Remote Sensing VIII, (2008).